ISSN 1070-4272, Russian Journal of Applied Chemistry, 2019, Vol. 92, No. 9, pp. 1244−1250. © Pleiades Publishing, Ltd., 2019.
Russian Text © The Author(s), 2019, published in Zhurnal Prikladnoi Khimii, 2019, Vol. 92, No. 9, pp. 1162−1169.

APPLIED ELECTROCHEMISTRY AND METAL CORROSION PROTECTION

Formation and Cathodic Reduction of Taurine Complexes with Zinc and Cobalt(II)

S. N. Gridchin[a,*] and R. F. Shekhanov[a]

[a] *Ivanovo State University of Chemistry and Technology, Ivanovo, Russia*
**e-mail: sergei_gridchin@mail.ru*

Received December 29, 2018; revised July 3, 2019; accepted July 3, 2019

Abstract—Stability constants of zinc and cobalt(II) complexes with Taurine were determined at 25°C and ionic strengths of 0.5, 1.0, and 1.5 (KNO_3). The thermodynamic stability constants were calculated. The processes in which zinc–cobalt alloys are electrodeposited onto 08kp steel from electrolytes with addition of Taurine and the physicochemical properties of the coatings were examined. It was shown that the ratio between the alloy components affect the chemical composition and microstructure of the coatings. The most homogeneous and finely crystalline structure is observed for zinc–cobalt alloy coatings obtained at a cathode current density of 1 A dm^{-2} from an electrolyte with zinc concentration twice that of cobalt. At these concentration conditions, zinc–cobalt alloy coatings with 15.1 at % Co were obtained. The kinetic patterns of deposition of zinc–cobalt alloys at temperatures of 25 and 50°C were demonstrated. A relationship between the chemical composition, microstructure, and corrosion rate of the zinc–cobalt coatings obtained was determined.

Keywords: stability constants, ionic strength, zinc–cobalt electrolytic alloys, polarization studies, corrosion resistance, chemical composition of an alloy, microstructure of coatings

DOI: 10.1134/S107042721909009X

Ferrous metals are commonly protected from corrosion by galvanic coating of articles with zinc, cadmium, and tin. Introduction of iron-subgroup metals (iron, cobalt, nickel) into anticorrosion coatings can make substantially longer their protective effect. The corresponding binary alloys provide a better corrosion protection of construction metals as compared with coatings composed of individual metals [1, 2]. At the same time, despite the permanently improving deposition technology of alloys of this kind, this problem remains one of the most complex and labor-consuming in electroplating. The electrolyte compositions being used have a number of important shortcomings. The coatings obtained frequently have a thickness insufficient for providing the necessary protective properties, poor adhesion to the base metal,and high internal stresses. Therefore, active studies are carried out all over the world, aimed to develop new effective electrolytes for obtaining galvanic alloys, revealing optimal electrodeposition modes and creating adequate physicochemical models describing the conditions of joint reduction of ions of metals being deposited [3, 4]. A promising area in the development of new solution compositions for electrodeposition of d-metals and alloys of these consists in using compounds that form soluble complexes with ions of metals being deposited, because electrolytes based on complex compounds can yield finely crystalline uniform-thickness coatings with high corrosion resistance [5–20]. One of the most effective ligands is taurine (2-amino ethane sulfonic acid, HL) [21, 22]:

$$H_2N–CH_2–CH_2–SO_3H.$$

Previously, the protolytic equilibria in aqueous solutions of this compound have been studied and the standard thermodynamic characteristics of the corresponding reactions have been determined [23]. The goal of our present study was to examine the complexation reactions with this amino acid with ions of zinc and cobalt(II) and the deposition processes of the zinc–cobalt electroplated alloy.

EXPERIMENTAL

The stability constants of taurine complexes with ions of zinc and cobalt(II) were determined by potentiometric titration at 25°C and ionic strengths of 0.5, 1.0, and 1.5 (KNO_3) inconformity with the procedure described in [24–26]. To determine the equilibrium concentration of hydrogen ion concentration, we measured the electromotive force of the circuit constituted by an ESL-43-07 glass electrode and EVL-1MZ saturated silver chloride electrode. The potential of the glass electrode was monitored with an R-363/3 potentiometer. A pH-340 pH meter–millivoltmeter served as the zero-instrument. The accuracy of potential measurement was ±0.1 mV. The titration was performed with standard potassium hydroxide solutions containing a "background" electrolyte to preclude a change in the ionic strength in the course of titration due to the dilution. A precisely measured volume of the taurine solution with a prescribed ionic strength was placed in a thermostated potentiometric cells. The initial concentration of the ligand was varied from 1.0×10^{-2} to 9.9×10^{-2} M at initial concentrations of metal ions of 7.2×10^{-3}–1.8×10^{-2} M. The temperature of the potentiometric cell was maintained with accuracy of ± 0.05. Prior to recording each titration curve, the potentiometric installation was calibrated against the standard solutions of HNO_3 and KOH, which contained potassium nitrate to create the necessary ionic strength.

The structure of the coatings was analyzed by atomic-force microscopy on a SOLVER 47 PRO instrument (tapping mode). The structure and composition of the alloys were examined with a tabletop scanning electron microscope with an integrated PHENOM PRO X system for energy-dispersive spectral analysis (EDS) and with a Tescan Vega 3 SBH scanning electron microscope with an attachment for elemental analysis. The coatings were deposited with an MPS-3005L-3 Matrix laboratory current source onto pretreated (degreased and activated) 08kp steel samples. The deposition process was performed at a temperature of 25°C and cathode current density of 1 A dm^{-2}. The coating thickness was 9 μm. The potentiodynamic cathodic polarization curves were recorded with a P30-J potentiostat at a temperature of 25°C at a potential sweep rate of 5 mV s^{-1}. The corrosion tests of the samples were performed in a 3% NaCl solution at a temperature of 25°C. The anodic dissolution curves of Zn–Co alloys and the cathodic curve of hydrogen reduction on 08kp steel were obtained at a potential sweep rate of 1 mV s^{-1}.

The Rozenfeld method [27] was used to obtain corrosion diagrams for zinc–cobalt alloys produced from oxalate electrolytes. The Rozenfeld method includes plotting of a cathodic polarization curve on which the potential of the base–metallic coating system is marked and used to determine the corrosion-element current.

RESULTS AND DISCUSSION

The stability constants of taurine complexes with zinc and cobalt(II) ions were calculated by PHMETR software [28] based on the principle of searching for the minimum of the criterion function F by varying in each iteration the values of log K to be determined

$$F = \Sigma(\log [H^+]_{j,\,\mathrm{exp}} - \log [H^+]^2_{j,\,\mathrm{calc}} \rightarrow \min, \qquad (1)$$

where $\log [H^+]_{j,\mathrm{exp}}$ and $\log [H^+]_j$, calc are the logarithms of the equilibrium functions, measured experimentally and calculated at current values of log K.

To minimize the criterion function, we used the modified Hook–Jives algorithm [29]. The equilibrium concentrations were calculated by the Brinkley method [30]. When the titration curves were processed the redox interaction reactions were taken into account together with the complexation processes. The dissociation constants of the amino acid under study have been determined previously [31]. The hydrolysis constants of metal ions were taken from [32]. The values found for the stability constants of zinc and cobalt(II) complexes with taurine at 25°C and ionic strengths I = 0.5, 1.0, and 1.5 (KNO_3) are listed in Table 1.

To determine the thermodynamic stability constants of the complexes with zinc and cobalt(II), we used the equation with a single individual parameter [33]:

$$\log K - A\Delta z^2 \sqrt{I} / (1+1.6\sqrt{I}) = \log K^\circ + bI, \qquad (2)$$

where log K and log $K°$ are, respectively, the logarithms of the concentration and thermodynamic stability constants; Δz^2, difference of squared ion charges; A, Debye–Hückel constant; I, ionic strength of the solution; and b, empirical constant characterizing the change in the dielectric constant of the medium near the ions.

The values obtained for log $K°$ by extrapolation of the corresponding concentration values to zero ionic strength are presented in Table 1.

Table 1. Decimal logarithms of the stability constants of zinc and cobalt(II) complexes with taurine at 25°C

Process	$I = 0.0$	$I = 0.5$	$I = 1.0$	$I = 1.5$
$Zn^{2+} + L^- = ZnL^+$	3.05 ± 0.10	2.47 ± 0.10	2.45 ± 0.09	2.49 ± 0.11
$ZnL^+ + L^- = ZnL_2$	2.51 ± 0.11	2.26 ± 0.11	2.33 ± 0.10	2.37 ± 0.12
$Zn^{2+} + 2L^- = ZnL_2$	5.56 ± 0.05	4.73 ± 0.05	4.78 ± 0.05	4.86 ± 0.05
$Co^{2+} + L^- = CoL^+$	2.86 ± 0.12	2.32 ± 0.12	2.36 ± 0.08	2.43 ± 0.09
$CoL^+ + L^- = CoL_2$	2.20 ± 0.14	1.93 ± 0.14	1.95 ± 0.11	1.99 ± 0.10
$Co^{2+} + 2L^- = CoL_2$	5.06 ± 0.08	4.25 ± 0.08	4.31 ± 0.07	4.42 ± 0.05

The processes of electrodeposition of zinc–cobalt alloys were examined with the electrolytes whose compositions are presented in Table 2.

The polarization curves obtained in electrolytes with various contents of metal ions are presented in Fig. 1. Polarization curves *1* and *2* show the limiting currents in the deposition of Zn–Co alloys. The polarization curves obtained in the electrolytes at 50°C have maxima increasing as the cobalt concentration grows at potentials in the range 600–650 mV. The probable reason is that the deposition of cobalt from these electrolytes is facilitated at an elevated temperature. The polarization and polarizability in electrolyte no. 3, i.e., at a double excess of zinc concentration over that of cobalt in the electrolyte (Table 2), is noticeably higher than that in electrolyte no. 1 both 25°C and at 50°C, which favors obtaining a more homogeneous finely crystalline structure of Zn–Co alloy coatings. The nearly 100% cathodic current efficiency favors a high deposition rate of the coatings and, consequently, a high efficiency in the output capacity of the electroplating processes.

As the content of cobalt in a coating increases, the deposition potential of the zinc–cobalt alloy is shifted to more positive values. The result is that the electromotive force of the corrosion element decreases and the corrosion current becomes lower (Fig. 2).

It was found that, at a cobalt content of 15.1 at % in the zinc–cobalt alloy, the corrosion rate of the zinc–cobalt alloy in the taurine electrolyte is 9.5 mA cm^{-2} (Table 3) and has the maximum value among the zinc–cobalt alloys under consideration. At a cobalt content of 46.1 at % in the alloy, the corrosion rate of a sample is at a minimum (0.5 mA cm^{-2}). At equal concentrations of zinc and cobalt in the electrolyte, the zinc–cobalt alloy

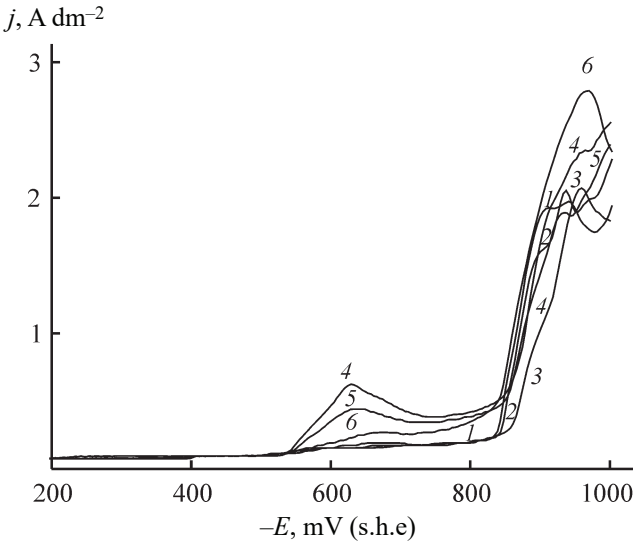

Fig. 1. Electrolyte: (*1*) no. 1, (*2*) no. 2, (*3*) no. 3, all at electrolyte temperature $T = 25$°C; (*4*) no. 1, (*5*) no. 2, (*6*) no. 3, all at electrolyte temperature $T = 50$°C.

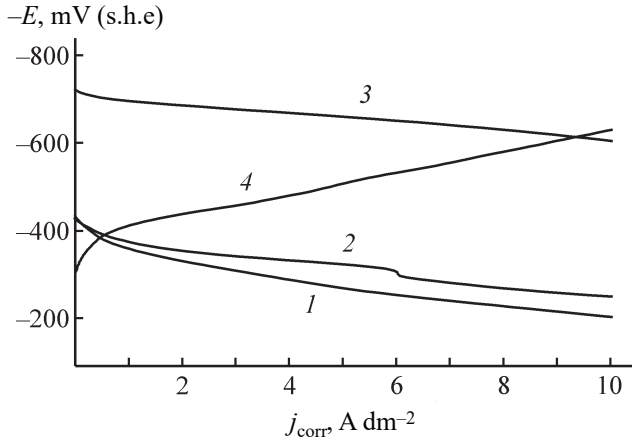

Fig. 2. Corrosion diagrams of zinc–cobalt alloy samples. Solution with 3% NaCl, $T = 25$°C. (*1–3*) Anodic curves for alloys deposited from the corresponding electrolytes at a temperature of 500°C; (*4*) cathodic curve on a steel electrode.

Table 2. Compositions of electrolytes for deposition of zinc–cobalt alloys

Composition	Content, M		
	no. 1	no. 2	no. 3
Taurine, $H_2NC_2H_4SO_3H$	0.40	0.40	0.40
Cobalt sulfate, $CoSO_4 \cdot 7H_2O$	0.10	0.08	0.05
Zinc sulfate, $ZnSO_4 \cdot 7H_2O$	0.05	0.08	0.10
Potassium chloride, KCl	1.68	1.68	1.68
pH	4.68	4.61	4.62

Table 3. Corrosion currents of steel samples coated with Zn–Co alloys from electrolyte nos. 1–3

Sample with a coating deposited from indicated electrolyte	Corrosion current density, mA cm^{-2}
No. 1	0.5
No. 2	0.7
No. 3	9.5

Table 4. Chemical composition of electroplated zinc–cobalt alloys

Electrolyte	Content, at %	
	Co	Zn
No. 1	46.1 ± 0.4	53.0 ± 0.4
No. 2	33.2 ± 0.4	66.8 ± 0.4
No. 3	15.1 ± 0.4	84.9 ± 0.4

contains 33.2 at % and the corrosion rate of the sample is 0.7 mA cm^{-2}.

The results obtained demonstrate that the lower corrosion rate is observed for zinc–cobalt coatings deposited from electrolyte nos. 1 and 2.

The atomic-force microscopy was used to examine the microstructure of Zn–Co coatings. The results obtained in examining the structure of the coatings and calculating the grain parameters of crystals of the zinc–cobalt alloys are presented in Tables 4 and 5.

Structural analysis of the coatings obtained at an anode current density of 1 A dm^{-2} (Fig. 3) and the results of crystallographic calculations suggest the zinc–cobalt alloy coating deposited from electrolyte no. 3 has the most homogeneous and finely crystalline structure. As expected, the content of cobalt in alloy grows with increasing concentration of its ions in solution. However, the structure of the alloys becomes more uniform and finely crystalline at lower cobalt concentrations (Fig. 4, electrolyte no. 3).

The Zn–Co alloy coating deposited from electrolyte no. 1 has an inhomogeneous structure, with regular rounded crystals with diameter of 1–2.5 μm and less present in the coating. The content of cobalt is 46.06 at % for alloys deposited from electrolyte no. 1, 33.23 at % for those deposited from electrolyte no. 2, and 15.08 at % for those formed from electrolyte no. 3, with zinc the rest.

Despite the substantial decrease in the corrosion rate for the first and second electrolytes, the zinc alloys that preserve the anodic nature of steel protection, i.e., those deposited from electrolyte nos. 3 and 2 will be considered the best acceptable.

Table 5. Grain parameters of crystals of zinc–cobalt alloys

Electrolyte no.	Area *S*, μm^2	Maximum height MaxZ, μm	Average height Z_{av}, μm	Parameter *P*, μm	Diameter *D*, μm	Length *L*, μm	Width *b*, μm
1	0.412	0.173	0.996	4.686	0.725	1.333	0.314
2	0.235	1.536	1.483	1.882	0.588	1.176	0.235
3	0.149	0.418	0.378	1.725	0.431	0.667	0.235

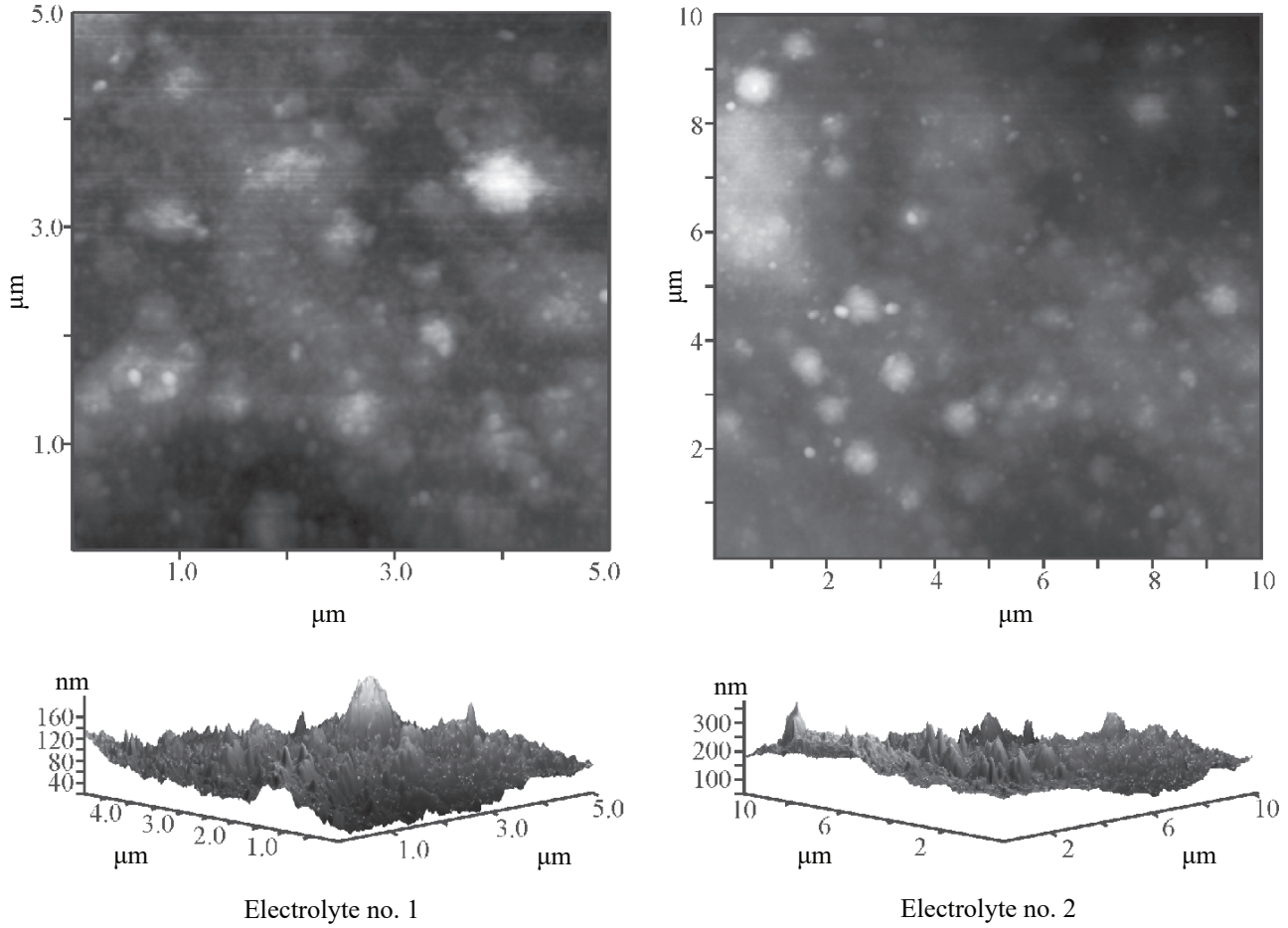

Fig. 3. Microstructure of Zn–Co coatings. Cathode current density 1 A dm^{-2}, temperature 25°C.

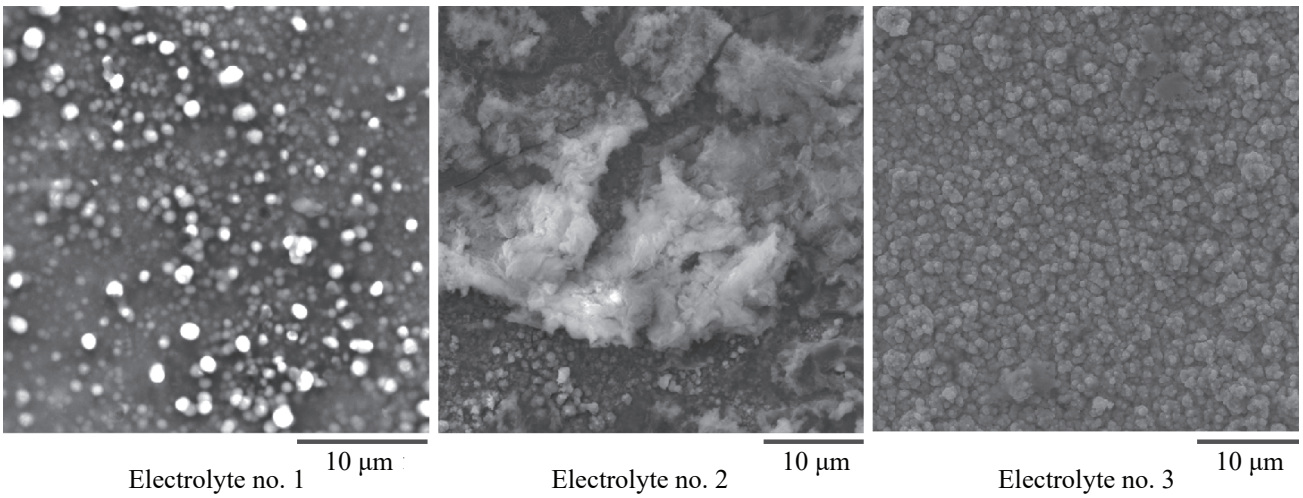

Fig. 4. Micrographs of Zn–Co alloys deposited from electrolyte nos. 1–3. Cathode current density 1 A dm^{-2}, temperature 25°C.

CONCLUSIONS

(1) The potentiometric method was used to determine the stability constants of zinc and cobalt(II) complexes with taurine at 25°C and ionic strengths of 0.5, 1.0, 1.5 (KNO_3). The thermodynamic stability constants were calculated.

(2) The polarization study demonstrated that, as the content of cobalt in a coating increases, its potential shifts

to more positive values. As a result, the electromotive force of the corrosion element and the corrosion current become lower.

(3) A low corrosion rate is observed for zinc-cobalt coatings deposited from electrolytes with equal concentrations of zinc and cobalt and also for zinc–cobalt alloys with high content of cobalt (46.1 at % Co). However, zinc alloys heavily alloyed with cobalt are characterized by a more positive potential than that of steel, which will lead to the loss of the anodic type of steel protection by zinc alloys. Therefore, the most promising in the authors' opinion are Zn–Co alloys with cobalt content of 15 to 33%.

(4) The content of cobalt in a coating grows with increasing concentration of cobalt ions in solution. However, more finely crystalline and structurally uniform coatings are formed at a relatively lower concentration of cobalt and also at the same concentrations of zinc and cobalt in the electrolyte. The most homogeneous and finely crystalline structure is observed for the zinc-cobalt alloy coating deposited from an electrolyte with zinc concentration twice the concentration of cobalt.

FUNDING

The study was carried out under the State assignment (base part), project no. 4.7104.2017/8.9.

CONFLICT OF INTEREST

The authors state that they have no conflict of interest to be disclosed in the present communication.

REFERENCES

1. Okulov, V.V., *Tsinkovanie. Tekhnika i tekhnologiya* (Zinc Plating. Equipment and Technology), Moscow: Globus, 2008, p. 104.
2. Bajat, J.B., Stevanovic, S.I., and Jokic, B.M., *J. Serb. Chem. Soc.*, 2011, vol. 76, no. 11, pp. 1537–1550. https://doi.org/10.2298JSC110331137B
3. Schlesinger, M. and Paunovic, M., *Modern Electroplating*, Hoboken: John Wiley & Sons, Inc., 2010, pp. 285–308.
4. Vinokurov, E.G. and Bondar', V.V., *Model'nye predstavleniya dlya opisaniya i prognozirovaniya elektroosazhdeniya splavov* (Model Concepts for Describing and Prognosticating the Electrodeposition of Alloys), Moscow: VINITI Ross. Akad. Nauk, 2009, pp. 88–136.
5. Vinokurov, E.G., *Russ. J. Appl. Chem.,* 2010, vol. 83, no. 2, pp. 258–262. https://doi.org/10.1134S1070427210020138
6. Evreinova, N.V., Shoshina, I.A., Naraev, V.N., and Tikhonov, K.I., *Russ. J. Appl. Chem.,* 2008, vol. 81, no. 9, pp. 1180–1183. https://doi.org/10.1134S1070427208070100
7. Taranina, O.A., Evreinova, N.V., Shoshina, I.A., Naraev, V.N., and Tikhonov, K.I., *Russ. J. Appl. Chem.,* 2010, vol. 83, no. 1, pp. 58–61. https://doi.org/10.1134S107042721001012X.
8. Kamel, M.M., Anwer, Z.M., Abdel-Salam, I.T., and Ibrahim, I.S., *Trans. IMF,* 2010, vol. 88, no. 4, pp. 191–197. https://doi.org/10.1179002029610X12696136822437
9. Gharahcheshmeh, M.H. and Sohi, M.H., *J. Appl. Electrochem.,* 2010, vol. 40, pp. 1563–1570. https://doi.org/10.1007s10800-010-0142-6
10. Ortiz-Aparicio, J.L., Meas, Y., Trejo, G., Ortega, R., Chapman, T.W., Chainet, E., and Ozil, P., *J. Appl. Electrochem.,* 2011, vol. 41, pp. 669–679. https://doi.org/10.1007s10800-011-0279-y
11. Lacnjevac, U., Jovic, B.M., and Jovic, V.D., *J. Electrochem. Soc.,* 2012, vol. 159, no. 5, pp. D310–D318. https://doi.org/10.11492.042205JES
12. Krasikov, A.V. and Krasikov, V.L., *Russ. J. Appl. Chem.,* 2012, vol. 85, no. 5, pp. 736–741. https://doi.org/10.1134S1070427212050096)
13. Hammami, O., Dhouibi, L., Bercot, P., and Rezrazi, E.A., *Canad. J. Chem. Eng.,* 2013, vol. 91, pp. 19–26. https://doi.org/10.1002cjce.21627
14. Sotskaya N.V., Sapronova, L.V., and Dolgikh, O.V., *Russ. J. Electrochem.,* 2014, vol. 50, no. 12, pp. 1134–1141. https://doi.org/10.1134S1023193514120106
15. Vidu, R., Perez-Page, M., Quach, D.V., Chen, X.Y., and Stroeve, P., *Electroanalysis,* 2015, vol. 27, pp. 2845–2856. https://doi.org/10.1002elan.201500247
16. Shekhanov, R.F., Gridchin, S.N., and Balmasov, A.V., *Surf. Eng. Appl. Electrochem.,* 2016, vol. 52, no. 2, pp. 152–156. https://doi.org/10.3103S1068375516020125
17. Shekhanov, R.F., Kuz'min, S.M., Balmasov, A.V., and Gridchin, S.N., *Russ. J. Electrochem*., 2017, vol. 53, no. 11, pp. 1274–1280. https://doi.org/10.1134S1023193517110131
18. Shekhanov, R.F., Gridchin, S.N., and Balmasov, A.V., *Russ. J. Electrochem*., 2018, vol. 54, no. 4, pp. 355–362. https://doi.org/10.1134S1023193518040079
19. Shekhanov, R.F., Gridchin, S.N., and Balmasov, A.V., *Prot. Met. Phys. Chem. Surf.,* 2017, vol. 53, no. 3, pp. 483–487. https://doi.org/10.1134S2070205117030224
20. Kahoul, A., Azizi, F., and Bouaoud, M., *Trans. IMF,* 2017, vol. 95, no. 2, pp. 106–113. https://doi.org/10.108000202967.2017.1265766
21. RF Patent 2 569 618 (publ. 2015).

22. RF Patent 2 603 526 (publ. 2016).
23. Gridchin, S.N., Shekhanov, R.F., and Pyreu, D.F., *Russ. J. Phys. Chem. A,* 2015, vol. 89, no. 2, pp. 341–343. https://doi.org/10.1134S0036024415020120
24. Gridchin, S.N., *J. Anal. Chem.,* 2007, vol. 62, no. 6, pp. 522–525. https://doi.org/10.1134S1061934807060044
25. Gridchin, S.N., *Russ. J. Phys. Chem. A,* 2016, vol. 90, no. 12, pp. 2499–2501. https://doi.org/10.1134S003602441612013X
26. Gridchin, S.N., *Russ. J. Gen. Chem.,* 2017, vol. 87, no. 12, pp. 2846–2851. https://doi.org/10.1134S1070363217120143
27. Rozenfel'd, I.L., *Korroziya i zashchita metallov* (Corrosion and Protection of Metals), Moscow: Metallurgiya, 1969, p. 105.
28. Borodin, V.A., Kozlovskii, E.V., and Vasil'ev, V.P., *Zh. Neorg. Khim.,* 1986, vol. 31, no. 1, pp. 10–16.
29. Himmelblau, D.M., Applied Nonlinear Programming, New York: McGraw-Hill Inc., 1972.
30. Vasil'ev, V.P., Borodin, V.A., and Kozlovskii, E.V., *Primenenie EVM v khimiko-analiticheskikh raschetakh* (Computers in Chemical Analytical Calculations), Moscow: Vysshaya shkola, 1993, pp. 81–101.
31. Gridchin, S.N., Shekhanov, R.F., Bychkova, S.A., *Konstanty ustoichivosti kompleksov kobal'ta(II) s taurinom i β-alaninom* (Stability constants of cobalt(II) complexes with taurine and β-alanine), *Izv. Vyssh. Uchebn. Zaved., Khim. Khim. Tekhnol.*, 2016, vol. 59, no. 3, pp. 95–96.
32. Nazarenko, V.A., Antonovich, V.P., and Nevskaya, E.M., *Gidroliz ionov metallov v razbavlennykh rastvorakh* (Hydrolysis of Metal Ions in Dilute Solutions), Moscow: Atomizdat, 1978. p. 46.
33. Vasil'ev, V.P., *Termodinamicheskie svoistva rastvorov elektrolitov* (Thermodynamic Properties of Electrolyte Solutions), Moscow: Vysshaya shkola, 1982, p. 267.